Research Article

Influence of Hydrostatic Pressure on the Formation of Voids in Gelled Crude Oil

Girma T. Chala*
International College of Engineering and Management, Muscat, Oman

Shaharin A. Sulaiman and Azuraien Japper-Jaafar
Department of Mechanical Engineering, Universiti Teknologi Petronas, Perak, Malaysia

Wan Ahmad Kamil Wan Abdullah
Department of Radiology, Hospital Universiti Sains Malaysia, Kelantan, Malaysia

* Corresponding author. E-mail: girma@icem.edu.om DOI: 10.14416/j.asep.2021.10.014
Received: 25 June 2021; Revised: 27 August 2021; Accepted: 7 September 2021; Published online: 29 October 2021

Abstract
Production of waxy crude oil from offshore fields has increased in the last decade. However, the operation is being challenged with the high wax content of crude oil that tends to precipitate at a lower temperature. This paper presents the effects of hydrostatic pressure on the voids formed in waxy crude oil gel. A flow loop rig that simulates offshore waxy crude oil transportation was used to produce the gel. A Magnetic Resonance Imaging of the 3-Tesla system was used to scan the gelled samples in horizontal and vertical pipes. The hydrostatic pressure effect was found to be the most significant near the pipe wall because a change in percent voids volume of 0.53% was observed in that region. In particular, the voids volume reduction was more pronounced in the lower half side of the pipe. The total volume of voids in the vertical pipe was lower than that in the horizontal pipe, and this suggests that the gel in the vertical pipe became denser due to the effects of the hydrostatic pressure. Conversely, the voids volume around the pipe core in the vertical pipe was higher when compared to that in the horizontal pipe. The change in voids volume near the pipe core and wall shrunk to a minimum and converged to 0.18% voids volume at a larger duration of the hydrostatic effect. Further, hydrostatic pressure was observed to have significant influences for the higher duration, making the void size distributed across and along the pipeline. However, it was found to have insignificant effects on voids size distribution for smaller duration. The findings of this study can help for a better understanding of voids formation in vertical pipelines that would further assist in developing a model predicting restart pressure accurately.

Keywords: Waxy crude oil, Hydrostatic pressure, Vertical pipe, Gas voids

1 Introduction

Production of waxy crude oil at offshore fields has increased in the last decade [1]. However, paraffin (waxes) cause significant flow assurance issues [2], [3]. Waxes constitute n-paraffins (C12–C35) with a higher tendency of deposition on pipe walls at lower temperatures [4]. A small percent of waxes in crude oil, as small as 2%, raises its pour point temperature [5]. In addition, Bai and Zhang found through microscopic observation that carbon number of waxes affected the entire waxy crude oil properties, which varied with the crude oil operating conditions and composition [6]. The presence of a higher amount of waxes would initiate precipitation and finally become a gel below the pour point temperature [7], [8].

Waxy-oil gel formation is usually inhomogeneous, principally due to shear and thermal histories encountered during cooling [9]. Rønningsen discussed methods of controlling wax deposition, including

monitoring and prediction of wax deposits [10]. It was highlighted in their study that wax removal is usually costly and time-consuming. In an effort to alleviate impacts of wax deposition, Bomba recommended the use of different techniques, namely, thermal, mechanical, chemical treatment, pour point depressant, and crystal modifier [11]. In a different work, Sarkat and Bhattacharya addressed that knowledge of pressure and temperature profiles of waxy crude oil could save the use of expensive chemical treatments [12].

Waxy crude oil reveals non-zero yield stress following sufficient cooling at offshore fields, and this would, in turn, affect the restart pressure [13]–[15]. Williams *et al.* studied the measurement of the yield stress of waxy crude oil subjected to variable cooling rates [16]. Pipe material, water cut, cooling rate, temperature, and bubble point affected the accuracy of the measurements. An increase in the restart pressure was also observed as the gel aged and became harder over time. Magda *et al.* presented a pressure profile of a clogged gel while restarting and showed that the gel fractured when the wall shear stress increased and exceeded the static yield stress, subsequently resulting in a cohesion stress reduction around the pipe walls [17]. The period of a shutdown was also noticed to have impacts on the restart pressure.

The thixotropic and compressibility behavior of waxy crude oil gel was observed, influencing the pressure needed to restart flows in pipelines [18]. Thixotropic behavior and compressibility of a waxy crude oil gel after shutdown were considered in the model developed by Davidson *et al.* [19]. Unlike other developed models for predicting restart pressure, they considered waxy crude oil as a compressible fluid. Their model revealed that oil compressibility effectively resulted in an enhanced oil flow rate. The compressibility of the waxy crude oil was also found significant during the initial transient flow at the restart [20]. Gabriel *et al.* developed a one-dimensional transient mathematical model for the Bingham fluid flow start-up in pipelines [21]. They concluded that low compressibility flow was usually exposed to oscillation. The pressure oscillation could lessen or even disappear in the event of a rise in compressibility.

Waxy crude oil practices thermal shrinkage during cooling, and this forms a void making a fluid unusually compressible [22], [23]. Local voids in the oil pipelines reduce the volume of waxy crude oil gel [24], [25]. Consequently, a significant reduction in the restart pressure could be resulted as a result of non-homogenous gel formation, as reported in the work of Wachs *et al.* [26]. Their numerical model showed that a flow of waxy crude oil could be resumed with a pressure well below that predicted using the conservative equation. Chala *et al.* used a 1 Tesla MRI to scan a gel in a pipe under static cooling in the preliminary flow loop rig developed [27]. They reported that voids formation in the gel had a direct relationship with the compressibility and yield stress needed to predict the restart pressure. In this line, the nature of voids needs to be understood to point out how void formation varies with different cooling scenarios. The hydrostatic pressure in the vertical pipe, for instance, had a direct influence on the restart pressure acting at the lower end of vertical pipelines. To the authors' knowledge, there have been no experimental results depicting the influence of hydrostatic pressure on the voids formed within the waxy crude oil gel. Therefore, the objective of this paper was to investigate the influence of hydrostatic pressure on the voids formed in vertical pipes and finally to be able to relate hydrostatic pressure with the voids at different locations in the pipe. This would help relate the effect of hydrostatic pressure with voids formed throughout pipelines at offshore fields, and this, in turn, facilitates accurate restart pressure prediction.

2 Materials and Methods

Figure 1 depicts a schematic diagram of a flow loop rig replicating waxy crude oil transportation at offshore fields. The rig mainly included a crude oil tank, a gear pump, a test section pipe, a chiller, and a centrifugal pump. The crude oil tank was equipped with a heater and a stirrer motor. To maintain the fluidity of the oil, it was kept above wax appearance temperature (WAT), 38.5 °C. The heater used had a capacity of heating the sample up to 100 °C, which was well above the WAT, and standardizes the flow by removing all the shear and thermal histories encountered during cooling. The test section pipe was immersed in a water bath simulating subsea pipelines. It was a detachable circular acrylic pipe of 1200 mm length and 30 mm diameter. The water bath had a rectangular shape with 29 cm height and a length of 135 cm. The width was 21 cm to hold 80 liters of water. A thermostat was installed inside the bath to read the temperature of cooled water (cooling

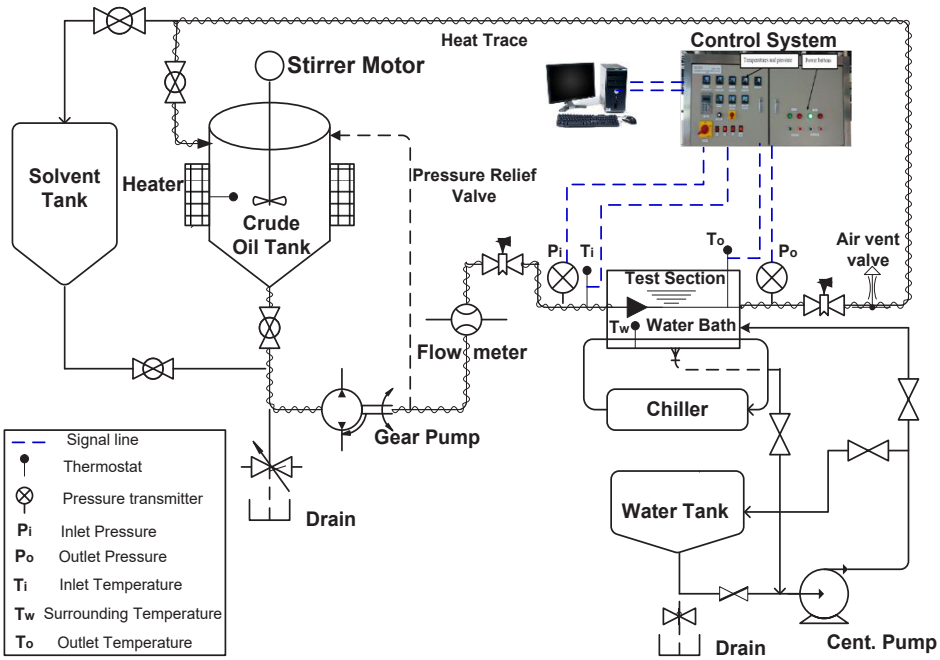

Figure 1: Experimental setup.

media). The upstream and downstream temperatures of waxy crude oil and the temperature of gelled crude oil in the acrylic pipe were recorded using a data logger.

Waxy crude oil underwent static cooling in the acrylic pipe until its end temperature, at which a consequent scanning was made. The gelled crude oil in the horizontal pipe was scanned in the 3T-Magnetic Resonance Imaging (3T-MRI) scanner. The scanned pipe was then made to stand vertically to observe the hydrostatic pressure effect due to an elevation difference. Following the pipe in a vertical stand, the pipe was then scanned at the same cross-section using the MRI. The durations of the pipe in the vertical stand were varied to understand the temporal change of voids formation as a result of hydrostatic pressure from the weight of the sample. As a result, short durations of the pipes in the vertical stand were selected, which were 10 to 25 min with 5 min interval between the experiments. In addition, the end temperatures of the samples were kept constant at 15 °C. The voids formed at the same cross-section in horizontal and vertical pipes were compared. The same procedure was applied for other sets of experiments cooled to the same end temperature, which would predict the hydrostatic pressure effects in the vertical pipe prior to a steady change. It would also predict voids in vertical pipes and relate gel strength with voids formed.

3 Magnetic Resonance Imaging System

The use of MRI in medical science is well known to scan soft tissues and other related parts in the human body [28]. A waxy crude oil with its constituents such as gel, water, and gas void made it suitable for the MRI scanner to detect the structure and formation of voids in the gel. A 3 T-MRI was used to scan pipe carrying gelled crude oil. Figure 2 shows the 3 T-MRI used to scan gelled samples in the horizontal and vertical pipes. Table 1 shows the main specifications of the 3 T-MRI used for the present study.

Table 1: Main specification of the 3T-MRI used

Lists	Descriptions
Magnetic system	Achieva 3.0 T
RF power and load cable	25000 W peak
Superconductivity	Liquid helium inside helium vessel
Air volume	400–500 [m^3/h]
Air cooling Min/Max pressure	58/90 Pa
Compressor	Cryo Compressor 3T REX

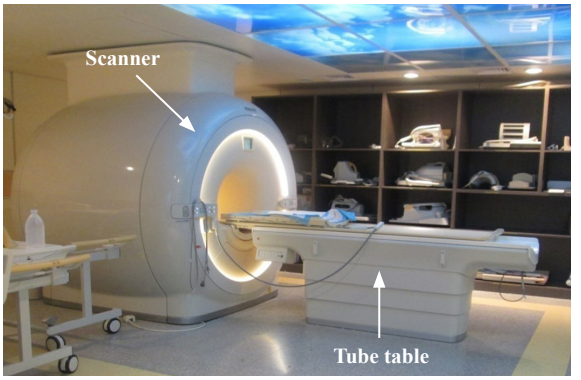

Figure 2: A 3 T-MRI used to scan gelled crude oil in pipes.

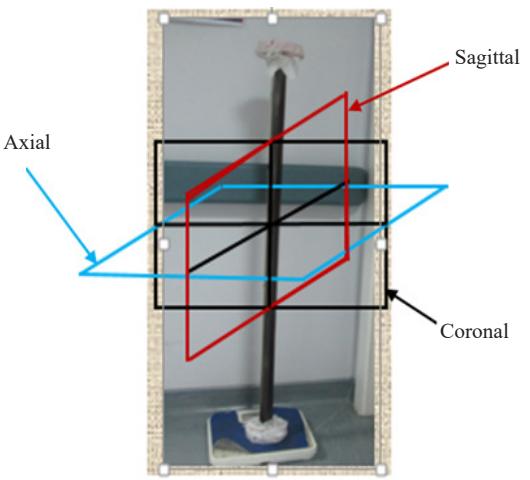

Figure 3: The three planes of MRI scan: Axial, Sagittal, and Coronal.

Figure 3 shows a photograph that defines the axial, sagittal, and coronal planes of the MRI, the common terms used by the operator in identifying the type of view of images of the scanned object. Images of gelled crude oil at the three planes were collected. Figure 4 shows an axial image at the midpoint of the scanned pipe. Two-dimensional images of 3 mm slice thickness and 0.5 mm gap were captured in three views. The axial view, which is also known as transverse view, shows images of the cross-sectional scanned pipe in the X-Y plane over the diameter of the pipe lying horizontally on the tube table of the MRI. The coronal view shows images of the scanned pipe along the X-Z plane. In contrast, the sagittal view shows images of the scanned pipe in the Y-Z plane.

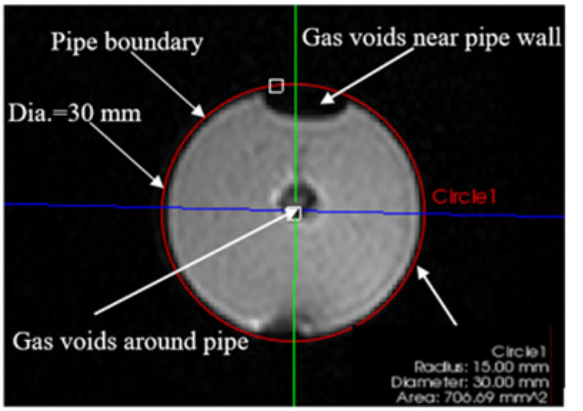

Figure 4: Cross-sectional axial image showing voids in T2 settings.

(a) (b)

Figure 5: Scanned crude oil gel: (a) 3D view and (b) cross-sectional view.

4 Results and Discussion

Voids volumes in the vertical and horizontal pipes were presented and compared. A 3D view showing the voids formed in the gel was generated from the 2D images numbering 100 in the axial view, 10 each in the sagittal and coronal views. Figure 5(a) shows a 3D view of the gel sample in the pipe. An axial image at the x-x cross-section is shown in Figure 5(b).

4.1 *Effects of hydrostatic pressure on the formation of voids*

Waxy crude oil in the acrylic pipe was cooled to an end temperature of 15 °C. The detachable horizontal pipe was scanned in the 3 T-MRI. The scanned pipe was left in a vertical stand for 10 min prior to another round of scanning to observe the effects of hydrostatic pressure on the voids formed. The voids areas at the same location in the horizontal and vertical pipes are compared. Figure 6(a) shows the distribution of void areas near the pipe wall in the horizontal and vertical pipes. The areas of voids formed in the vertical pipe

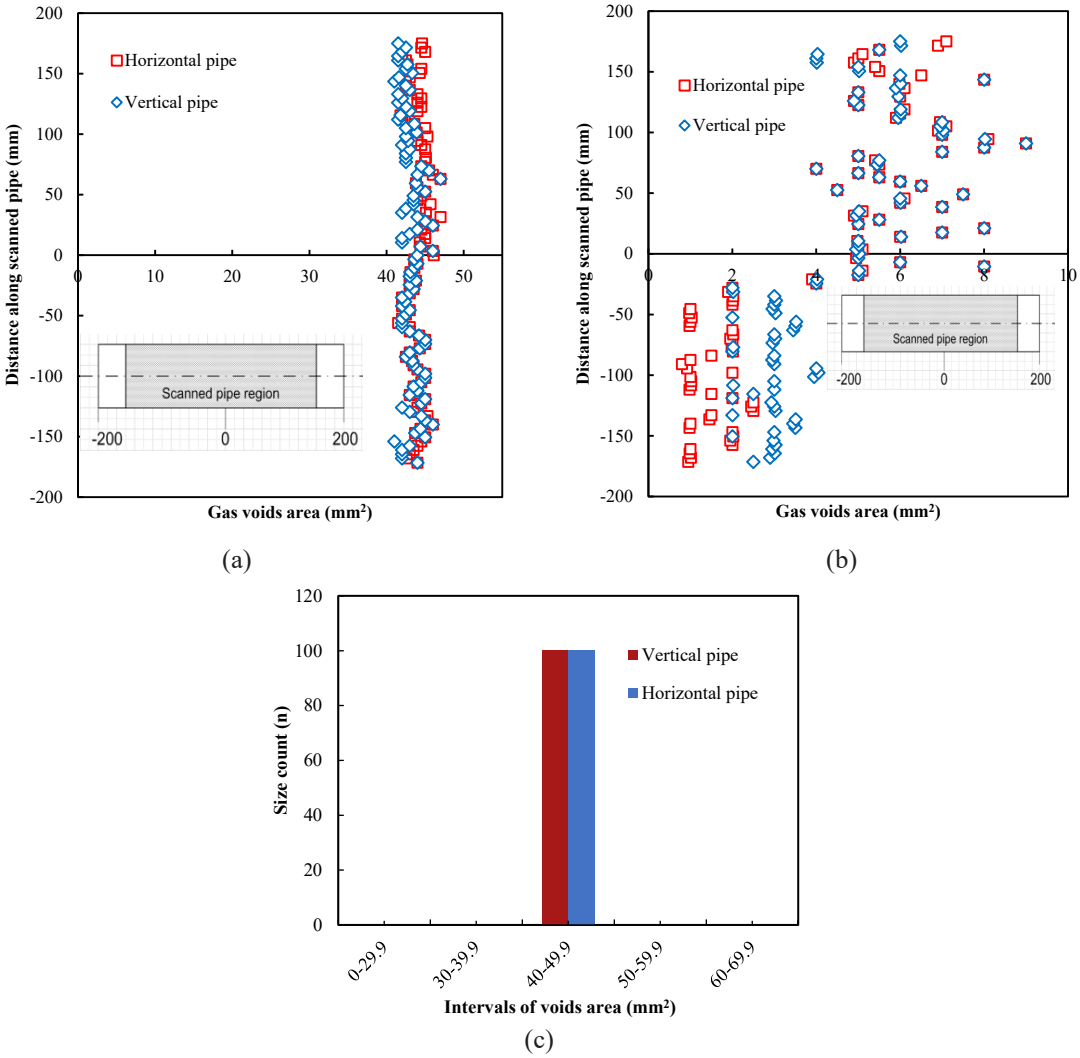

Figure 6: Voids area: (a) near pipe wall, (b) around pipe core, and (c) voids size distribution when duration was 10 min.

are shown to be lower as compared to those in the horizontal pipe. The reduction in voids volume was significant at the top side of the pipe compared to that below the midpoint of the pipe.

Gas voids around pipe core in the horizontal and vertical pipes are shown in Figure 6(b). The voids areas were slightly bigger in the vertical pipe as opposed to that in the pipe wall. In particular, the change in voids area was higher below the midpoint of the pipe due to the significant effects of hydrostatic pressure around this region. Further, it was observed that voids areas around the pipe core were found smaller than that near the pipe wall. This is mainly due to the higher temperature of crude oil around the pipe center than near the pipe wall. Rukthong, *et al.* also observed lower temperature at the pipe wall with a higher influence of conduction and convection heat transfer as opposed to that at the center [29]. Moreover, Chala *et al.* noticed a drop in temperature towards the pipe wall, making a viscosity to be higher near the pipe wall [30]. The same observation was also reported elsewhere [31], [32]. Size distributions of voids near the pipe wall in the horizontal and vertical pipelines were analyzed to investigate the arrangement of voids formation due to the hydrostatic pressure.

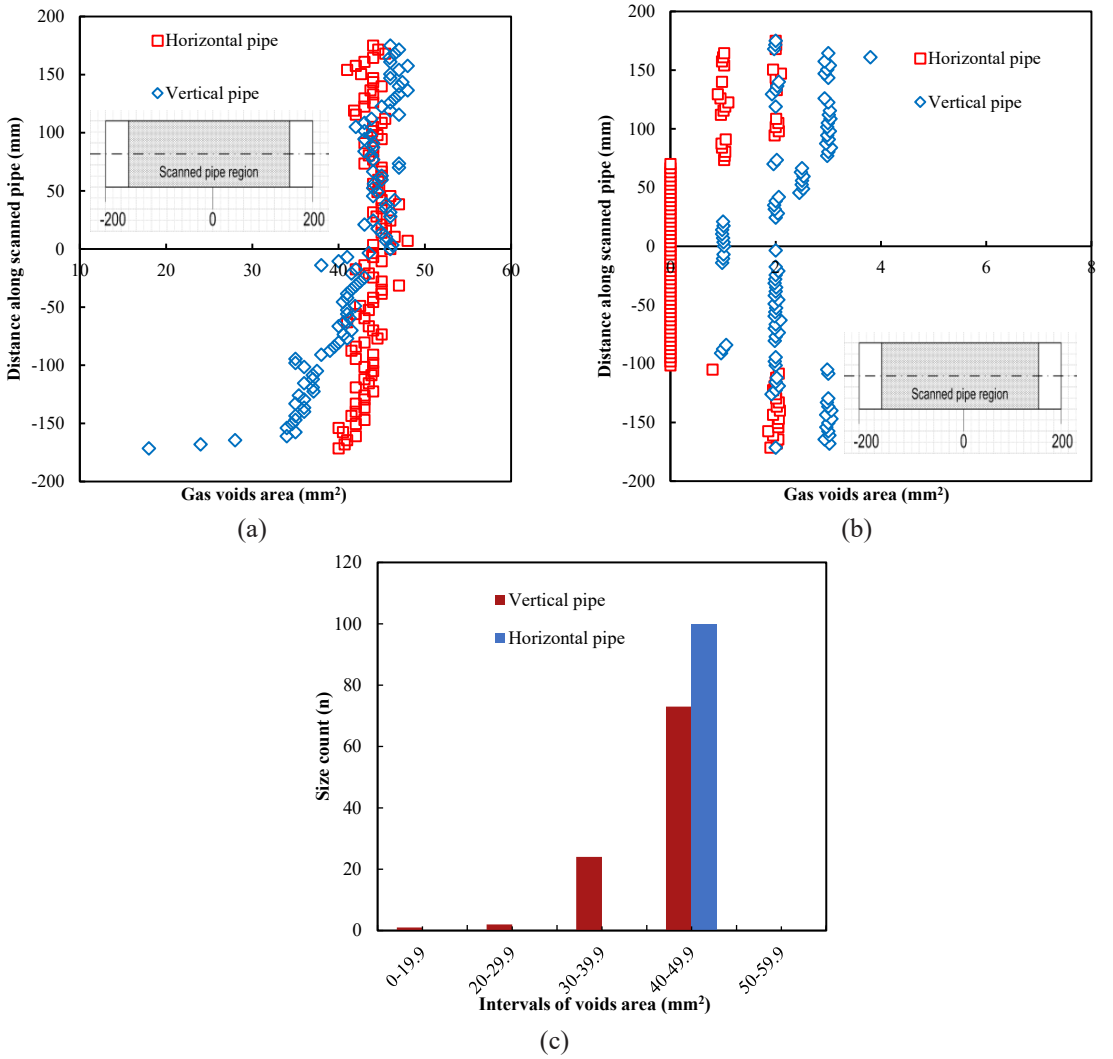

Figure 7: Voids area: (a) near pipe wall, (b) around pipe core and (c) voids size distribution when duration was 15 min.

Figure 6(c) shows voids size distribution near the pipe wall in the vertical and horizontal pipes. It was observed that all cross-sections of the pipeline had similar voids size count in size ranging between 40 and 49.9 mm^2 that showed no effects of hydrostatic pressure on voids size distribution for the smaller duration.

Another set of experiments cooling waxy crude oil to an end temperature of 15 °C was conducted. The hydrostatic pressure was acting for 15 min prior to the second round of scanning. Figure 7(a) and (b) show voids area near the pipe wall and core, respectively. The voids near pipe wall in a vertical pipe were found plausibly lower at the bottom end of the scanned pipe than voids in the horizontal pipe. The lower voids area in the vertical pipe predicts a higher strength of the sample at this region. The difference became minimal at the midpoint of the pipe and became slightly higher at the top end. The minimum voids area of 18 mm^2 was measured at the bottom end of the vertical pipe near the pipe wall, while voids area in the horizontal pipe was 40 mm^2, showing the significant influence of hydrostatic pressure. In contrast, voids areas at the pipe core in the vertical pipe were higher throughout the pipe distance than that in the horizontal pipe. Figure 7(c) shows voids size distribution near the pipe wall. Higher voids size distribution was observed as a result of

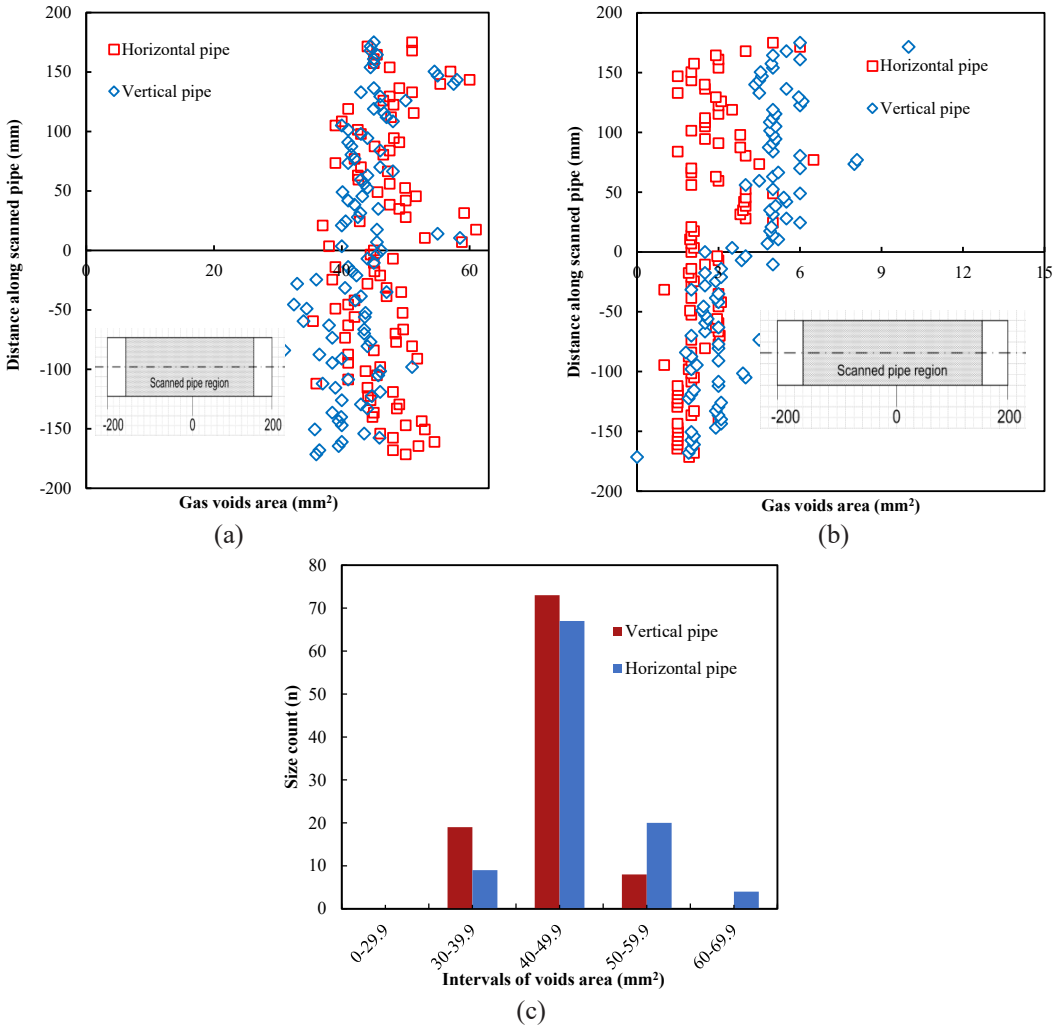

Figure 8: Voids area: (a) near pipe wall, (b) around pipe core and (c) voids size distribution when duration was 20 min.

hydrostatic pressure. Moreover, the distribution was also higher in the vertical pipe with a bigger size count in four different size ranges between 0 to 49.9 mm^2. The bigger voids size distribution was anticipated by the hydrostatic pressure acting profoundly below the mid-point of the pipeline.

Cooling of waxy crude oil was made to an end temperature of 15 °C. The hydrostatic pressure acted in the vertical pipe for 20 min. Voids areas distributed around pipe wall in the horizontal and vertical pipes is shown in Figure 8(a). The voids area around the bottom end in the vertical pipe was significantly lower than that in a horizontal pipe, where 54.5 mm^2 cross-sectional voids area was measured in the vertical pipe, while it was 40 mm^2 in the horizontal pipe. An insignificant change of voids area between horizontal and vertical pipes was observed at the top end of the pipes. The effects became higher around the midpoint of the scanned pipe, and a significant change of voids area was observed at 17.5 mm along the pipe, at which voids area of 61 mm^2 was measured in the vertical pipe, while it was 45.5 mm^2 in the horizontal pipe. The distribution of voids areas around pipe core in the horizontal and vertical pipes is shown in Figure 8(b). Unlike pipe walls, the voids areas in the vertical pipe were higher than that in the horizontal pipe, almost all over the cross-section along the pipe. The difference in voids areas between horizontal and vertical pipes was higher above the midpoint

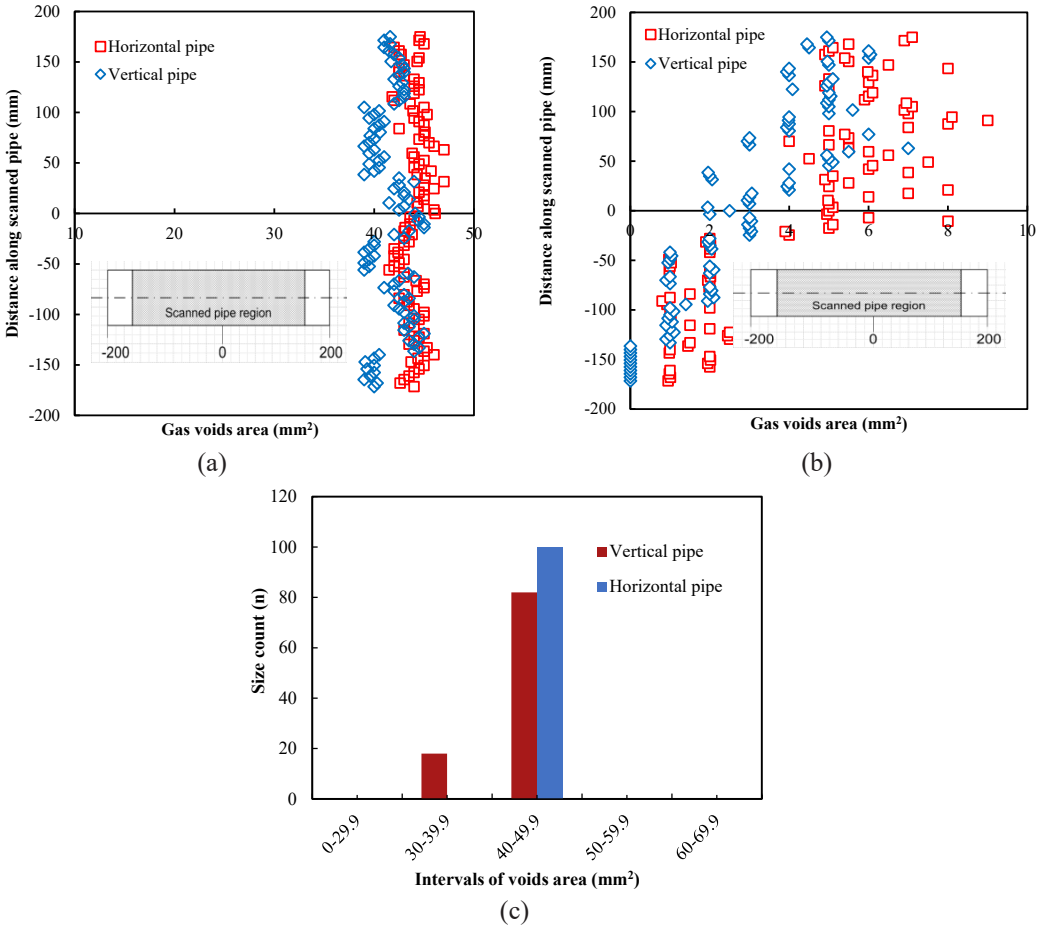

Figure 9: Gas voids area: (a) near pipe wall, (b) around pipe core and (c) voids size distribution when duration was 25 min.

of the scanned pipe, mainly at the top end of the pipes.

Voids size distributions near the pipe wall in the horizontal and vertical pipelines were investigated. Figure 8(c) shows size count versus intervals of voids areas in the horizontal and vertical pipes. A vertical pipe had its 73 cross-section with voids size concentrating in the intervals of 40–49.9 mm^2, 19 in the interval between 30–39.9 mm^2 and the remaining 8 cross-sections had voids size in the interval between 50–59.9 mm^2, showing lower non-uniform size distribution when compared to that in the horizontal pipe. Hydrostatic pressure was also observed, reducing the size distribution; however, the size of voids area was still lower for hydrostatic pressure.

Waxy crude oil was cooled statically to an end temperature of 15 °C. The scanned pipe was in the vertical stand for 25 min to observe the effect of hydrostatic pressure on the temporal variation of the void formed. Figure 9(a) shows voids area around pipe wall in horizontal and vertical pipes. The voids formed in the vertical pipe were found lower along with the pipe distance both at the lower and upper parts of the pipe. Voids areas in vertical and horizontal pipes were almost similar at the midpoint of the pipes, around, which a little higher void area in the vertical pipe was also observed at –14 mm. A significant change of voids areas was observed around the bottom of the pipes. The void area at the bottom end in the horizontal pipe, for instance, was 44 mm^2 while it was 40 mm^2 in the vertical pipe. Figure 9(b) depicts the distribution of voids areas around the pipe core in the vertical and horizontal pipes. At this elevated duration, voids areas in the horizontal pipe were found to be higher than that in the vertical pipe. The voids size distribution near the pipe wall in the vertical and

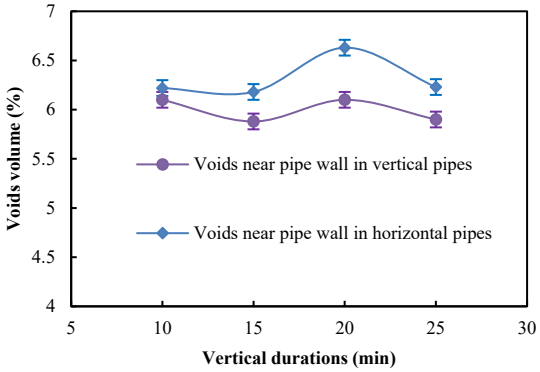

Figure 10: Voids volume near pipe wall in vertical and horizontal pipes.

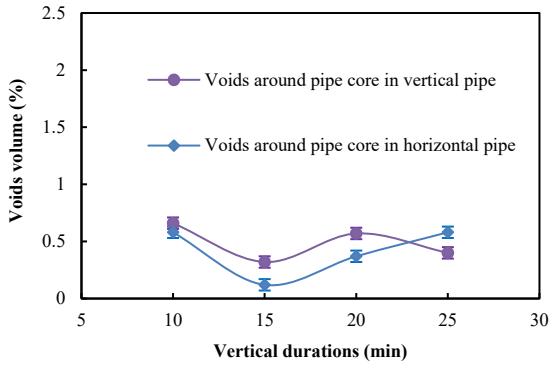

Figure 11: Voids volume around pipe core in vertical and horizontal pipes.

horizontal pipes is depicted in Figure 9(c). The voids size distribution was higher in the vertical pipe than that in the horizontal pipe, again indicating the influence of hydrostatic pressure by distributing voids sizes along and across the pipeline. Further, it was observed that the distribution was in two ranges scales along with minimizing the voids areas, which in one way reduces the size of the voids and distributes it more in other views.

4.2 *Comparison of voids volume near pipe wall in the vertical and horizontal pipe*

The resulting voids volume near pipe wall in the horizontal and vertical pipes due to hydrostatic pressure was compared. Figure 10 shows the variation of voids volume near the pipe wall in the horizontal and vertical pipes versus vertical durations. Voids volume in the horizontal pipe is higher than that in the vertical pipe. The difference in voids volume was observed to increase slightly with vertical durations. However, the maximum change of voids was observed at 20 min vertical duration with the percentage of voids volume reduced from 6.63% to 6.1%. Voids volumes in horizontal and vertical pipes were 6.23% and 5.9%, respectively, at an elevated duration of 25 min.

4.3 *Comparisons of voids volume around pipe core in the horizontal and vertical pipes*

Figure 11 shows the percent of voids volume around pipe core in the horizontal and vertical pipes for various durations. Voids volume in the vertical pipe was higher than that in the horizontal pipe at lower durations, which was opposite to what was observed near the pipe wall. The voids volumes in the vertical and horizontal pipes were almost similar between 20 and 25 min vertical durations. A higher voids volume in the horizontal pipe was then calculated at 25 min vertical durations, at which voids volume decreased from 0.58% to 0.4%, with a reduced voids volume of 0.18% in the vertical pipe.

4.4 *Comparisons of total voids volume in the horizontal and vertical pipes*

The total voids volume in the horizontal and vertical pipes is compared at all vertical durations. Figure 12 shows the total voids volume in both pipes. Voids volumes were almost similar in the vertical and horizontal pipes at the lowest duration, which indicates the insignificant effects of hydrostatic pressure. The hydrostatic pressure effects then increased as the change in voids volume between the two pipes increased with duration. Total voids volume in the horizontal pipe was higher than that in the vertical pipe at all durations. The lower voids volume found in the vertical pipe would predict a denser gel with higher yield stress compared to the gel sample in the horizontal pipe due to hydrostatic pressure.

4.5 *A combined comparisons of voids volume in the vertical and horizontal pipes*

A combined comparison of voids volume in a vertical and horizontal pipe was made. Figure 13 shows a combined comparison of voids volume at three different

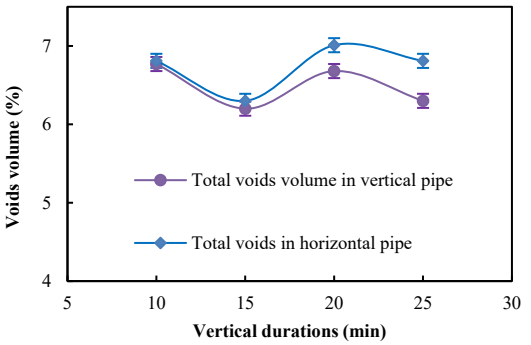

Figure 12: Total voids volume in vertical and horizontal pipes.

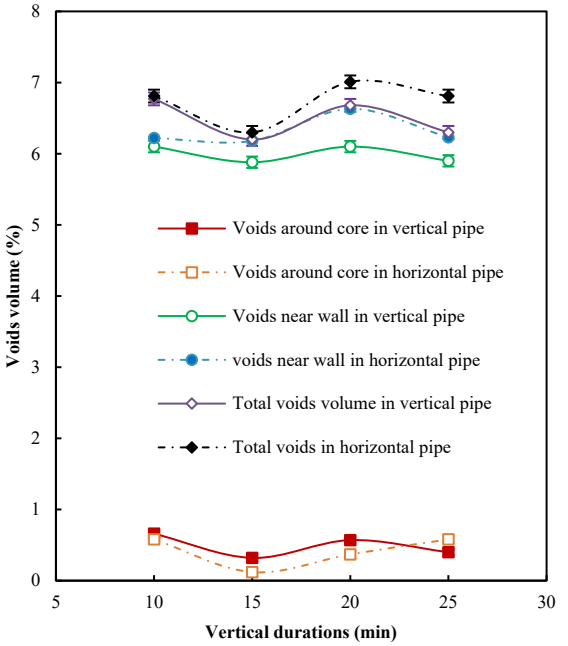

Figure 13: Comparisons of voids volume in vertical and horizontal pipes.

regions. At minimum hydrostatic effect duration, the percentages of voids volume near pipe wall in the horizontal and vertical pipes were calculated to be 6.18% and 5.88%, respectively. In contrast, percentages of voids volume around pipe core in the vertical and horizontal pipes were 0.319% and 0.11%, respectively. The voids volumes near the pipe wall and in the entire pipe in the horizontal pipe were higher than that in the vertical pipe, showing denser gel due to hydrostatic pressure. The trend was opposite around the pipe core.

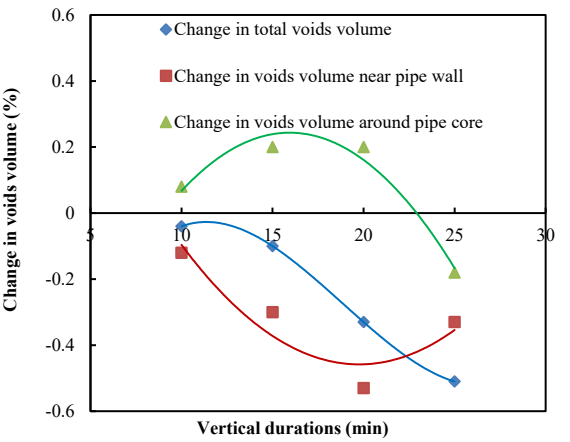

Figure 14: Change in voids volume between horizontal and vertical pipes.

4.6 *Comparison of voids volume changes between horizontal and vertical pipes*

Comparisons between changes of voids volume in vertical and horizontal pipes were made to outline the transient effect of hydrostatic pressure. Figure 14 shows the change in voids volume between horizontal and vertical pipes over all regions. The total percentage of voids in the horizontal pipe was calculated to be 6.3%, and a total of 6.2% void volume was observed in the vertical pipe after a 15 min hydrostatic effect, with a 0.1% decline of the pipe. An increased hydrostatic effect duration led to an increased total voids volume change between horizontal and vertical pipes. The change in voids volume near pipe wall increased and finally decreased to a smaller value. The same reflection was observed around the pipe core, in which the change in voids volume between vertical and horizontal pipes increased and decreased to only 0.18%.

5 Conclusions

This paper presents the influence of hydrostatic pressure on the formation of voids in vertical pipes. A flow loop rig replication offshore fields were used to prepare gel for the 3 T-MRI, which scanned voids within the gelled crude oil. Voids volume in the horizontal and vertical pipes and the change in voids volume between the horizontal and vertical pipes were compared. Hydrostatic pressure made total voids

volume in the vertical pipe lower than that in the horizontal pipe, indicating denser gel in the vertical pipe. Voids volume near the pipe wall was also larger in the horizontal pipe, with a maximum calculated change in voids volume of 0.53%, making the hydrostatic effects stronger at that region. A completely different observation was noted around the pipe core, at which a higher voids volume was formed in the vertical pipe, especially above the midpoint of the scanned pipe, forming a relatively insignificant lighter gel. The change in voids volume near the pipe wall and core shrunk to a minimum and converged to 0.18% at a longer hydrostatic effects duration. Furthermore, hydrostatic pressure was found to have insignificant effects on voids size distribution for the smaller duration; however, it was observed to have significant influences for the higher duration, making the void size to be distributed across and along pipelines. This study recommends that the hydrostatic pressure effect in vertical pipes needs to be included while predicting an accurate restart pressure with more focus given to voids near a wall of the pipelines.

Acknowledgements

The authors would like to thank the Universiti Teknologi PETRONAS for the support provided.

References

[1] M. Seyyedattar, S. Zendehboudi, and S. Butt, "Technical and non-technical challenges of development of offshore petroleum reservoirs: Characterization and production," *Natural Resources Research*, vol. 29, no. 3, pp. 2147–2189, 2020.

[2] A. K. Mehrotra, S. Ehsani, S. Haj-Shafiei, and A. S. Kasumu, "A review of heat-transfer mechanism for solid deposition from "waxy" or paraffinic mixtures," *The Canadian Journal of Chemical Engineering*, vol. 98, no. 12, pp. 2463–2488, 2020.

[3] F. Alnaimat and M. Ziauddin, "Wax deposition and prediction in petroleum pipelines," *Journal of Petroleum Science and Engineering*, vol. 184, 2020, Art. no. 106385.

[4] N. Sa-ngawong, T. Kangsadan, K. Cheenkachorn, N. Inwong, and A. Mahittikul, "Study on local composition of binary n-alkane for precise estimation of wax disappearance temperature," *Applied Science and Engineering Progress*, vol. 14, no. 2, pp. 271–283, 2021, doi: 10.14416/j.asep.2020.02.002.

[5] G. T. Chala, S. A. Sulaiman, and A. Japper-Jaafar, "Flow start-up and transportation of waxy crude oil in pipelines-A review," *Journal of Non-Newtonian Fluid Mechanics*, vol. 251, pp. 69–87, 2018.

[6] C. Bai and J. Zhang, "Effect of carbon number distribution of wax on the yield stress of waxy oil gels," *Industrial & Engineering Chemistry Research*, vol. 52, no. 7, pp. 2732–2739, 2013.

[7] A. Japper-Jaafar, P. T. Bhaskoro, and Z. S. Mior, "A new perspective on the measurements of wax appearance temperature: Comparison between DSC, thermomicroscopy and rheometry and the cooling rate effects," *Journal of Petroleum Science and Engineering*, vol. 147, pp. 672–681, 2016.

[8] Z. Liu, Y. Li, W. Wang, G. Song, Z. Lu, and Y. Ning, "Wax and wax–hydrate deposition characteristics in single-, two-, and three-phase pipelines: A review," *Energy & Fuels*, vol. 34, no. 11, pp. 13350–13368, 2020.

[9] S. A. Sulaiman, B. K. Biga, and G. T. Chala, "Injection of non-reacting gas into production pipelines to ease restart pumping of waxy crude oil," *Journal of Petroleum Science and Engineering*, vol. 152, pp. 549–554, 2017.

[10] H. P. Rønningsen, "Production of waxy oils on the norwegian continental shelf: Experiences, challenges, and practices," *Energy & Fuels*, vol. 26, no. 7, pp. 4124–4136, 2012.

[11] J. G. Bomba, "Offshore pipeline transport of waxy crude oils," presented at the Offshore South East Asia Show, Singapore, Jan. 28–31, 1986.

[12] B. Sarkar and A. Bhattacharya, "Transportation of waxy crude through pipeline systems: Analysis of some critical design parameters," presented at the First International Offshore and Polar Engineering Conference, Edinburgh, The United Kingdom, Aug. 11–16, 1991.

[13] G. Ovarlez, S. Cohen-Addad, K. Krishan, J. Goyon, and P. Coussot, "On the existence of a simple yield stress fluid behavior," *Journal of Non-Newtonian Fluid Mechanics*, vol. 193, pp. 68–79, 2013.

[14] M. Fossen, T. Øyangen, and O. J. Velle, "Effect of the pipe diameter on the restart pressure of a gelled waxy crude oil," *Energy & Fuels*, vol. 27, no. 7, pp. 3685–3691, 2013.

[15] G. T. Chala, S. A. Sulaiman, A. Japper-Jaafar, and W. A. K. W. Abdullah, "Impacts of cooling rates on voids in waxy crude oil under quiescent cooling mode," *Applied Mechanics and Materials*, vol. 799–800, pp. 62–66, 2015.

[16] T. M. Williams, J. J. C. Hsu, and H. L. Patterson, "Measurement of break away yield stress of waxy crude oil and pipeline restart system design," presented at the Offshore Technology Conference, Texas, USA, May 6–9, 1996.

[17] J. J. Magda, A. Elmadhoun, P. Wall, M. Jemmett, M. D. Deo, K. L. Greenhill, and R. Venkatesan, "Evolution of the pressure profile during the gelation and restart of a model waxy crude oil," *Energy & Fuels*, vol. 27, no. 4, pp. 1909–1913, 2013.

[18] S. Mortazavi-Manesh and J. M. Shaw, "Thixotropic rheological behavior of maya crude oil," *Energy & Fuels*, vol. 28, no. 2, pp. 972–979, 2014.

[19] M. R. Davidson, Q. Dzuy Nguyen, C. Chang, and H. P. Rønningsen, "A model for restart of a pipeline with compressible gelled waxy crude oil," *Journal of Non-Newtonian Fluid Mechanics*, vol. 123, no. 2–3, pp. 269–280, 2004.

[20] S. A. Sulaiman, G. T. Chala, and M. Z. Zainur, "Experimental investigation of compressibility of waxy crude oil subjected to static cooling," *Journal of Petroleum Science and Engineering*, vol. 182, 2019, Art. no. 106378.

[21] G. M. De Oliveira, L. L. V. da Rocha, A. T. Franco, and C. O. Negrão, "Numerical simulation of the start-up of Bingham fluid flows in pipelines," *Journal of Non-Newtonian Fluid Mechanics*, vol. 165, no. 19–20, pp. 1114–1128, 2010.

[22] G. T. Chala, S. A. Sulaiman, A. Japper-Jaafar, and W. A. K. W. Abdullah, "Effects of cooling regime on the formation of voids in statically cooled waxy crude oil," *International Journal of Multiphase Flow*, vol. 77, pp. 187–195, 2015.

[23] B. Abedi, M. J. P. Miguel, P. R. de Souza Mendes, and R. Mendes, "Startup flow of gelled waxy crude oils in pipelines: The role of volume shrinkage," *Fuel*, vol. 288, 2021, Art. no. 119726.

[24] A. Shafquet, I. Ismail, A. Japper-Jaafar, S. A. Sulaiman, and G. T. Chala, "Estimation of gas void formation in statically cooled waxy crude oil using online capacitance measurement," *International Journal of Multiphase Flow*, vol. 75, pp. 257–266, 2015.

[25] S. Majidi and A. Ahmadpour, "Thermally assisted restart of gelled pipelines: A weakly compressible numerical study," *International Journal of Heat and Mass Transfer*, vol. 118, pp. 27–39, 2018.

[26] A. Wachs, G. Vinay, and I. Frigaard, "A 1.5D numerical model for the start up of weakly compressible flow of a viscoplastic and thixotropic fluid in pipelines," *Journal of Non-Newtonian Fluid Mechanics*, vol. 159, no. 1–3, pp. 81–94, 2009.

[27] G. T. Chala, S. A. Sulaiman, A. Japper-Jaafar, W. A. K. W. Abdullah, and M. M. M. Mokhtar, "Gas void formation in statically cooled waxy crude oil," *International Journal of Thermal Sciences*, vol. 86, pp. 41–47, 2014.

[28] T. Defraeye, V. Lehmann, D. Gross, C. Holat, Els Herremans, P. Verboven, B. E. Verlindenb, and B. M. Nicolai, "Application of MRI for tissue characterisation of 'Braeburn' apple," *Postharvest Biology and Technology*, vol. 75, pp. 96–105, 2013.

[29] W. Rukthong, W. Weerapakkaroon, U. Wongsiriwan, P. Piumsomboon, and B. Chalermsinsuwan, "Integration of computational fluid dynamics simulation and statistical factorial experimental design of thick-wall crude oil pipeline with heat loss," *Advances in Engineering Software*, vol. 86, pp. 49–54, 2015.

[30] G. T. Chala, C. Chan, and H. Sadig, "Temperature profile and its effects on the location of lower denser substance in waxy crude oil: A numerical study," *Advanced Science Letters*, vol. 24, no. 11, pp. 8880–8884, 2018.

[31] A. Tavakoli and M. Baktash, "Numerical approach for temperature development of horizontal pipe flow with thermal leakage to ambient," *International Journal of Modern Engineering Research*, vol. 2, pp. 3784–3794, 2012.

[32] G. T. Chala, S. A. Sulaiman, A. Japper-Jaafar, and W. A. K. W. Abdullah, "Temporal variation of voids in waxy crude oil gel in the presence of temperature gradient," *Chemical Engineering Communications*, vol. 207, no. 10, pp. 1403–1414, 2020.